Acta Geodyn. Geomater., Vol. 10, No. 3 (171), 285–291, 2013
DOI: 10.13168/AGG.2013.0028

ORIGINAL PAPER

GLOBAL AND REGIONAL SEASONAL VARIATIONS OF THE GEOID DETECTED BY GRACE

Jan KOSTELECKÝ [1, 2] *, Aleš BEZDĚK [3] and Jaroslav KLOKOČNÍK [3]

[1] *Research Institute of Geodesy, Topography and Cartography, p.r.i., Ústecká 98, CZ-250 66 Zdiby*
[2] *Institute of Geodesy and Mine Surveying, Faculty of Mining and Geology, TU Ostrava, 17. listopadu 15, CZ-708 33 Ostrava Poruba*
[3] *Astronomical Institute, Academy of Sciences of the Czech Republic, Fričova 298, CZ-251 65 Ondřejov*
**Corresponding author's e-mail:* kost@fsv.cvut.cz

(*Received* January 2013, *accepted* April 2013)

ABSTRACT
Since 2002, the US-German GRACE (Gravity Recovery and Climate Experiment) mission has been providing a precise survey of the Earth's time-variable gravity field, with unprecedented temporal and spatial sampling. GRACE time-variable gravity fields provide a means of measuring the temporal and spatial variations of mass redistribution within the Earth system. The GRACE mission has started a new era in studying a series of geophysical problems ranging from deep Earth structure to tracking mass redistribution on and near the surface of the Earth. Time variability of the gravity field presented here is based on the transformation of "monthly gravity field models" to the geoid. We show the changes caused by the global water cycle and land hydrology.

KEYWORDS: GRACE mission, seasonal variations, geoid

1. INTRODUCTION

In the first decade of the 21st century, three space geodesy missions took place, focused on the study of Earth's gravity field. The first of these was CHAMP (Reigber et al., 2002). CHAMP completed its mission and re-entered the Earth's atmosphere on 19 September 2010, after 10 years (operational lifetime was 5 years) and after 58277 orbits; it was aimed at studying the detailed structure of the gravity and magnetic fields of the Earth. It was followed by the GRACE mission (Tapley et al., 2004), equipped for the low-low satellite-to-satellite tracking, launched in 2002, primarily aimed at studying the detailed structure and temporal variations of the Earth's gravity field. And finally the satellite GOCE (ESA, 1999; Floberghagen et al., 2011), launched in 2009, working till now, whose purpose is to measure the second derivatives of the gravitational field of the Earth and thus to study the fine structure of the Earth's gravity field.

Of these three missions only the two, CHAMP and GRACE, are focused on the temporal variations of the gravity field. For a recent review of results from the GRACE mission, see, e.g., Cazenave and Chen (2010), Chambers and Schröter (2011) or Landerer and Swenson (2012).

2. DETERMINATION OF THE SURFACE OF THE GLOBAL GEOID

The gravitational field of the Earth is characterized by the so-called *gravitational potential* V, a scalar, which is a function of the position only. By taking the directional derivative of this potential, one obtains the vector of the gravitational *acceleration*. The most common expression for the gravitational potential is its representation by a spherical harmonic series

$$V(r,\Phi,\lambda)=\frac{GM}{r}\cdot \left[1+\sum_{l=2}^{\infty}\sum_{m=0}^{l}\left(\frac{a_e}{r}\right)^l P_{lm}(\sin\Phi)\left(C_{lm}\cos m\lambda+S_{lm}\sin m\lambda\right)\right] \tag{1}$$

where $V(r,\Phi,\lambda)$ is the potential, which is a function of geocentric spherical coordinates r,Φ,λ, a_e is radius of an Earth reference ellipsoid, $P_{lm}(\sin\Phi)$ are the associated Legendre functions, C_{lm},S_{lm} are the amplitudes of cosine and sine terms (Stokes parameters), l is degree and m order, which basically divide Earth's surface into sectors, limited by meridians and parallels. The summation over l theoretically extends to infinity, in a given specific case we use only relatively small values of (l, m).

A set of parameters C_{lm},S_{lm} defines a *model of the gravitational field*. These parameters are determined by applying the Gauss method of least squares (LS) to solve the dynamic problem of space geodesy, which is based on the (non-linear) relationship between observations and the parameters of the gravitational field. Observations are of different types. In the case of the CHAMP satellite, its position is determined through the GPS technology (high-low satellite-to-satellite tracking). In the case of the GRACE mission, the positions of the two satellites are measured by the GPS technology, in addition to their mutual distance, precisely measured using a micro-wave link.

One has two possibilities for monitoring the temporal variations of the gravity field. The first possibility is to express the time variations of individual parameters C_{lm}, S_{lm}. The number of these parameters is very high and the result would not be instructive. It is much more illustrative to show the time variations via the geoid surface fluctuations, because these changes respond to the mass changes. In the following, we will follow this approach.

We will use the term global geoid to indicate the geoid surface, representing the geoid over the whole Earth, which is determined by a set of Stokes parameters, limited by a certain finite degree l_{max} and order m_{max}, which are, in turn, "smoothed" to a certain extent.

We will start with the expression for the gravitational potential (1), symbolically rewritten as

$$V(r,\Phi,\lambda) = \frac{GM}{r} f(r,\Phi,\lambda). \quad (2)$$

The geoid is defined as an equipotential surface of the constant **gravity potential** W,

$$W = V + Q , \quad (3)$$

where Q is the centrifugal potential,

$$Q = \frac{1}{2}\omega^2 r^2 \cos^2 \Phi = Q(r,\Phi) , \quad (4)$$

ω is the rotation rate of the Earth. On substituting to Eq. (3), we may formally write

$$W = \frac{GM}{r}\left[f(r,\Phi,\lambda,Q)\right]. \quad (5)$$

The geoid is the surface of the constant potential, let us denote it by W_{geoid}. Then, in a similar way, Eq. (5) could be expressed as

$$W_{geoid} = \frac{GM}{r_{geoid}}\left[f(r_{geoid},\Phi,\lambda,Q)\right]. \quad (6)$$

For its radius vector from (6) we have

$$r_{geoid} = \frac{GM}{W_{geoid}}\left[f(r_{geoid},\Phi,\lambda,Q)\right]. \quad (7)$$

From this expression for the radius vector, it is obvious that for a known value of W_{geoid}, we can determine r_{geoid} and that this is feasible in an iterative way.

To a certain extent, we could select an arbitrary value for W_{geoid}, but if we want to comply with the traditional definition, which says that the geoid is an equipotential surface coinciding with the mean ocean level (with dynamic ocean topography removed), it is possible to determine W_{geoid} within the framework of the so-called **scale factor R_0.**

Let us denote (see Zhongolovich, 1957, or Burša and Pěč, 1993, part 2.5.4)

$$R_0 = \frac{GM}{W_{geoid}} \quad (8)$$

From this definition it is clear that R_0 represents the radius of a sphere having the potential W_{geoid}. It is then possible to rewrite Eq. (7) as

$$r_{geoid} = R_0\left[f(r_{geoid},\Phi,\lambda,Q)\right] \quad (9)$$

and finally

$$R_0 = r_{geoid}\left[f(r_{geoid},\Phi,\lambda,Q)\right]^{-1}. \quad (10)$$

If using, e.g., satellite altimetry or GPS, we succeed in "mapping" the mean ocean level, i.e. to map r_{geoid}. Then we can determine the scale factor R_0 and from its value we can get W_{geoid} through Eq. (8).

The current value of the gravity potential of the global geoid reads (Petit et al., 2010):

$$W_{geoid} = 62\,636\,856.0 \pm 0.5\ m^2.s^{-2}$$

Thanks to new geodetic satellite missions it is possible to create models of the global geoid in short time intervals (monthly solutions). Based on these models, it is possible to estimate temporal variations of the geoid surface (they are caused mainly by hydrological effects).

The other access to the solution of the problem is via "height anomaly" N (see Holmes and Pavlis, 2006):

$$N = \frac{T}{\gamma} + \frac{Dgb}{\gamma} H \quad (11)$$

where N is the height of the geoid above the reference ellipsoid, T is the disturbing potential, γ is the normal gravity at the computing point, Dgb is Bouguer anomaly and H is the sea-level height of the computing point.

3. DATA – "MONTHLY MODELS" OF EARTH'S GRAVITY FIELD FROM THE MISSION GRACE

The mission GRACE (Gravity Recovery And Climate Experiment) is based on a system of two satellites, whose distance is measured by a K-band radio frequency link (Tapley et al., 2004). The position of both satellites is determined by means of

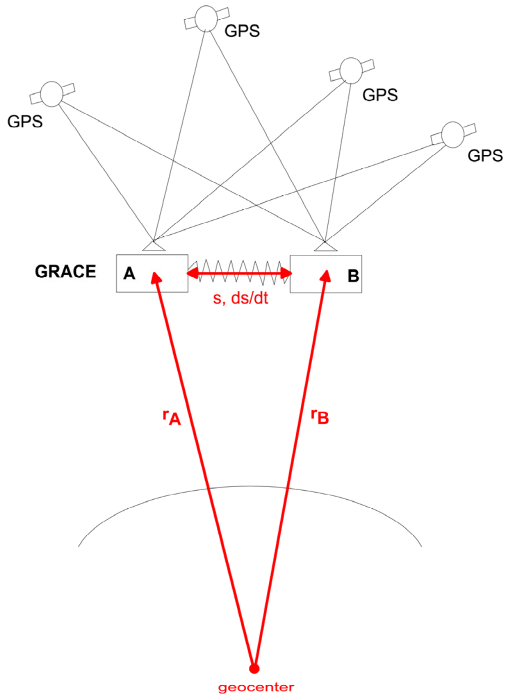

Fig. 1 Principle of the GRACE mission measurements is based on the determination of
a) position vectors (determined from GPS) and
b) measurement of distance and its change between both the satellites.

GPS, see Figure 1. From GPS, we know the position vectors $\boldsymbol{r_A}$ and $\boldsymbol{r_B}$, from the relative measurement we know *s* and *ds/dt*. From the solution of the dynamic problem of satellite geodesy, it follows that all these quantities are also functions of the Earth's gravity field parameters C_{lm}, S_{lm}. By solving the inverse problem, we can determine the individual Stokes parameters C_{lm}, S_{lm} and obtain a set, which we then call the model of Earth's gravitational field. The determination of one set of the Stokes parameters up to a certain degree *l* and order *m* requires longer time series of observations, currently the optimum time interval used is one month – therefore, these models are called "monthlies". (There are attempts to use shorter time series of observations).

Models created from the GRACE data, covering short periods of time (see below), are published by these institutions:

- CSR – Center of Space Research, Texas, USA (l_{max} = 60, period of data collection is app. 30 days)
- GFZ – GeoForschungsZentrum, Potsdam, Germany (l_{max} = 90, period of data collection is app. 30 days)
- JPL – Jet Propulsion Laboratory, Pasadena, USA (l_{max} = 60 or 90, period of data collection is app. 30 days)
- CNES/GRGS – Toulouse, France (l_{max} = 50, period of data collection is only10 days)
- ITG – University Bonn, Germany (l_{max} = 120, period of data collection is app. 30 days)
- DMT-1 – TU Delft, Netherlands (l_{max} = 120, period of data collection is app. 30 days)
- AIUB – Astronomical Institute University of Berne, Switzerland (l_{max} = 60, period of data collection is app. 30 days)

These models (in the form of Stokes parameters and using different data formats) together with the supporting documentation are available at: http://icgem.gfz-potsdam.de/ICGEM/.

In our analysis we used the models of AIUB, CSR, GFZ (name "EIG") and CNES/GRGS (name "GRGS"). We used the AIUB "non-filtered" data, for other models we took the so-called "filtered" data.

Our aim is to express the geoid height variations during a specified time period in the form of graphs. The following steps are needed:

- To convert the "monthly" models to a normalized form.
- To transform the gravity field parameters to the geoid.

  This operation requires two steps:
- To define a field of points at which the geoid heights will be computed.
- To compute these geoid heights, related to a specified "monthly" gravity field model. For this purpose, it is possible to use "harmonic_synth" program (Holmes and Pavlis, 2006) or another relevant computer program, which is capable of computing the Legendre associated functions up to the required high degree and order. The result is the set of geoid heights above a reference ellipsoid (here the ellipsoid GRS80 was used).

4. GRAPHICAL REPRESENTATION OF TEMPORAL VARIATIONS OF THE GEOID

There are different methods to express the temporal variations:

(a) to express differences between two geoid models at two different epochs;

(b) to express the maximum values of the differences for the studied time period;

(c) to express seasonal variation – amplitudes and phases of the annual and semiannual terms with respect to a fixed epoch;

(d) to approximate variations for selected regions (Amazon basin, India, Greenland and Siberia) by "unharmonic analysis" (published by P. Vaníček in 1971 and last described in Kostelecký and Karský, 1987) to determine secular trends and main periodicities.

Table 1 Amplitudes of seasonal (one year) variations of geoid in millimetres.

	AIUB	CSR	EIG	GRGS
Amazon basin	10.2	9.1	8.1	8.5
India	7.8	5.9	5.3	5.3
Greenland	2.8	2.0	0.8	1.2
Siberia	4.6	4.3	3.3	3.4
Dispersion of input data	2.6	0.8	0.6	1.0

Table 2 Values of the secular trends of the geoid changes (and their standard deviations) in millimetres per year.

	AIUB	CSR	EIG	GRGS
Amazon basin	–0.24 ± 0.15	0.42 ± 0.05	0.50 ± 0.02	0.28 ± 0.02
India	–0.58 ± 0.14	0.12 ± 0.03	0.14 ± 0.03	0.11 ± 0.02
Greenland	–0.61 ± 0.23	**–3.13 ± 0.04**	**–2.00 ± 0.03**	**–2.18 ± 0.04**
Siberia	1.56 ± 0.18	–0.22 ± 0.06	0.43 ± 0.03	0.04 ± 0.02

All this will be done globally for the whole Earth as well as for the Central Europe. As a specific example we chose the monthly models produced by CSR (Center of Space Research, Texas, USA) with a maximum degree and order (l, m) = 60. We used the CSR Release-04 monthly solutions, from which the non-tidal variations in the atmosphere and oceans were removed; all the processing details are given in Bettadpur (2007).

Method (a): In Figure 2 we show the maximum value of the "half-seasonal" variations. The difference is caused by a hydrological effect, which comprises the influence of tropical rains on the hydrological resources.

Method (b): In Figure 3, there are the maximum values of the difference in the geoid height for one and a half year period. Apart from the variations in the tropical belt, there is a distinct change in Siberia and western Canada caused by the change in the snow cover. In Figure 4 we show the same quantities as in Figure 3, but for the period 2004–2012. Besides the mentioned areas, there is a larger change in the hydrology of Greenland.

Method (c): For the specified period 2004–2012, locally (in each point) we approximated the geoid heights by annual and semi-annual terms. The resulting amplitudes are shown in Figure 5. Compared to the previous cases, the variations are now "smoother", the amplitudes reach about a half of the previous values. Values of amplitudes for different models for the four selected regions are shown in Table 1. Taken into account the dispersion of the data (see the last row of Table 1) the agreement of the results from different processing centres is quite good.

Method (d): For the specified period 2003–2010 we approximated the geoid heights by the secular and periodic terms. These approximations were made for the regions of Amazon basin, India, Greenland and Siberia. The results are depicted in Figure 6. (*Time scale in Figure 6 and Figure 8 uses the so called "Modified Julian Date" which is the continuous count of days, used in astronomy*). The values of the secular trends are shown in Table 2. If we compare the results, we must keep in mind that the data from AIUB are not filtered and thus they have a greater dispersion. A greater secular trend of the geoid height, about –2.5 mm/year, may be seen only for Greenland, it is caused by ice melting.

The regional variations were computed for the Central Europe. The maximum differences of the values over the period 2004–2012 are depicted in Figure 7. In the central part (Czech Republic, CZ), the values reach 7–8 mm.

For the Geodetic observatory Pecný at Ondřejov, CZ (φ = *49° 55'* and λ = *14° 47'*), we have the absolute gravity data measured by the absolute gravimeter FG5, No. 215 of MicroG–Solution, with an accuracy of 2 μGal. The variations in the gravity values are caused mainly by the local and global hydrological effect (Pálinkáš et al., 2013). After converting the values of the measured gravity difference to the height difference we can compare these data with the variations obtained from the monthly models. Figure 8 shows the time series from both the sources. The phases of the two signals correspond rather well, the amplitudes of the absolute gravimeter manifest the dominant influence of the local hydrology.

5. CONCLUSIONS

Time variations of the Earth's gravity field were studied using the GRACE data expressed as the geoid height variations. A combination of the monthly solutions describes the seasonal variations in the geoid height with high fidelity. The variations are caused by the mass transport, especially by the hydrological effects. These variations reach values of a few millimetres. It is legitimate to ask about the credibility of detecting such small values, when we know that the precision of the geoid itself, as approximated by the Stokes parameters, is at the level of a few centimeters (for degree and order 60). The reason is given by the

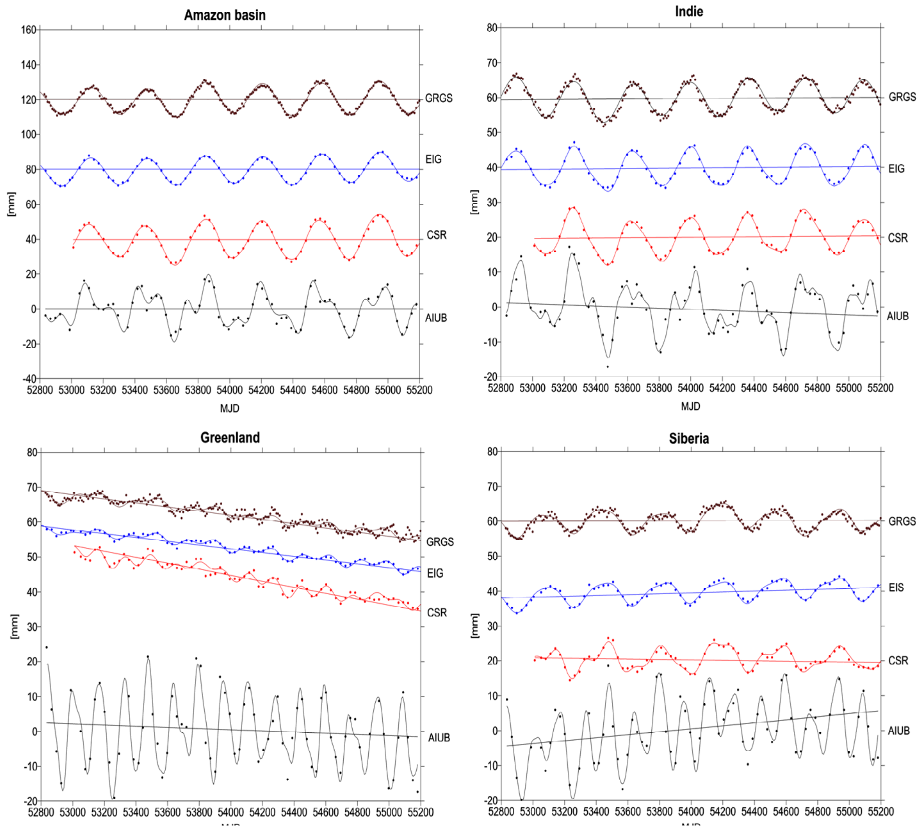

Fig. 6 Change of the geoid height for selected regions of the Earth based on different solutions (MJD 52800 = 10 June 2003, MJD 55200 = 4 January 2010).

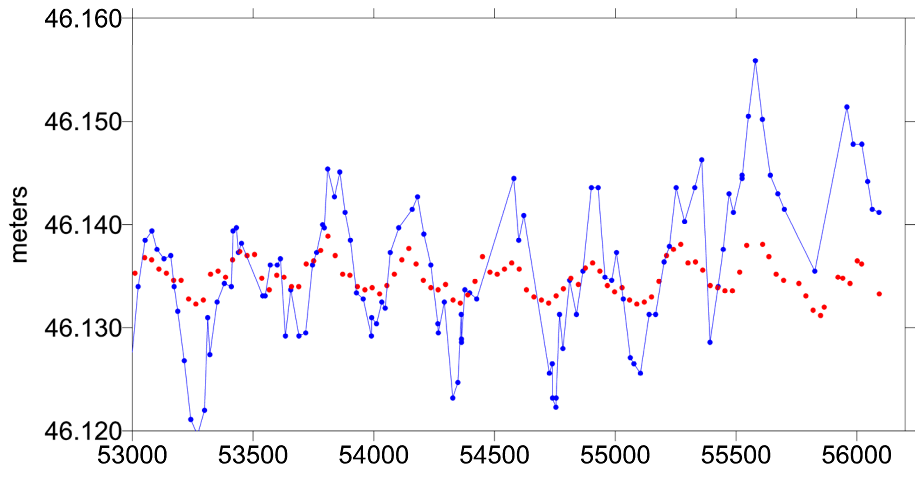

Fig. 8 Time variations of the geoid height at the GOPE station – *points* are from GRACE monthly solution (CSR Texas), *line* displays changes derived from the absolute gravimeter FG5 No 215 solution (MJD 53000 = 27 December 2003, MJD 56000 = 14 March 2012).

strong correlation between the individual monthly solutions (see the evident seasonal sinusoids in Fig. 6), which makes the results more precise by an order of magnitude, when we compute their differences.

ACKNOWLEDGMENT

This contribution was made possible thanks to the project of the European Regional Development Fund (ERDF), project "NTIS – New Technologies for Information Society", European Centre of Excellence, CZ.1.05/1.1.00/02.0090 and project TB01CUZK006 of TA CR. Special thanks are to Dr. V. Pálinkáš (Geodetic Observatory Pecný) for the data given us via the project LM2010008 – CzechGeo EPOS. As for the Astronomical Institute, this work was supported by the project RVO: 67985815 and by the project No. 13-36843S of Czech Science Foundation (GACR).

REFERENCES

Bettadpur, S.: 2007, UTCSR Level-2 processing standards document, for Level-2 product release 0004. GRACE 327-742 (CSR-GR-03-03), CSR, Austin, USA.

Burša, M. and Pěč, K.: 1993, Gravity Field and Dynamics of the Earth, Springer Verlag, Berlin, Heidelberg.

Cazenave, A. and Chen, J.: 2010, Time-variable gravity from space and present-day mass redistribution in the Earth system. Earth and Planetary Science Letters 298, 263–274. DOI: 10.1016/j.epsl.2010.07.035

Chambers, D.P. and Schröter, J.: 2011, Measuring ocean mass variability from satellite gravimetry. Journal of Geodynamics 52, 333–343. DOI: 10.1016/j.jog.2011.04.004

ESA: 1999, Gravity Field and Steady-State Ocean Circulation Mission, report for mission selection of the four candidate Earth Explorer missions. ESA SP-1233(1).

Floberghagen, R., Fehringer, M., Lamarre, D., Muzi, D., Frommknecht, B., Steiger, C., Pineiro, J. and da Costa, A.: 2011, Mission design, operation and exploitation of the gravity field and steady-state ocean circulation explorer mission. Journal of Geodesy 85, 749–758. DOI: 10.1007/s00190-011-0498-3

Holmes, S.A. and Pavlis, N.K.: 2006, A FORTRAN program for very-high-degree harmonic synthesis (Version 05/01/2006). http://earth info.nga.mil/GandG/wgs84/gravitymod/new_egm/new_egm.html

Kostelecký, J. and Karský, G.: Analysis of 1970 - 1983 circumzenithal measurements. Bull. Astron. Inst. Czechosl. 38, 1987, 16 pp.

Landerer, F.W. and Swenson, S.C.: 2012, Accuracy of scaled GRACE terrestrial water storage estimates. Water Resources Research 48, W04531. DOI: 10.1029/2011WRO11453

Pálinkáš, V., Lederer, M., Kostelecký, J. jr., Šimek, J. Mojzeš, M., Ferianc, D. and Csapó, G.: 2013, Analysis of the repeated absolute gravity measurements in the Czech Republic, Slovakia and Hungary from the period 1991-2010 considering instrumental and hydrological effects. Journal of Geodesy 87, 29–42. DOI: 10.1007/s00190-012-0576-1

Petit, G., Luzum, B., et al.: 2010, IERS Conventions (2010). Verlag des Bundesamts für Kartographie und Geodäsie, Frankfurt am Main.

Reigber, C., Lühr, H. and Schwintzer, P.: 2002, CHAMP mission status. Advances in Space Research 30, 129–134. DOI: 10.1016/S0273-1177(02)00276-2

Tapley, B. D., Bettadpur, S., Watkins, M. and Reigber, C.: 2004, The gravity recovery and climate experiment: Mission overview and early results. Geophys Res Lett 31, 9607–9613. DOI: 10.1007/s00190-012-0576-1

Zhongolovich, I.D.: 1957, Earth's gravity potential. Bull. Inst. Teoret. Astronomii, tom VI, No 8(81), 505–523, (in Russian).

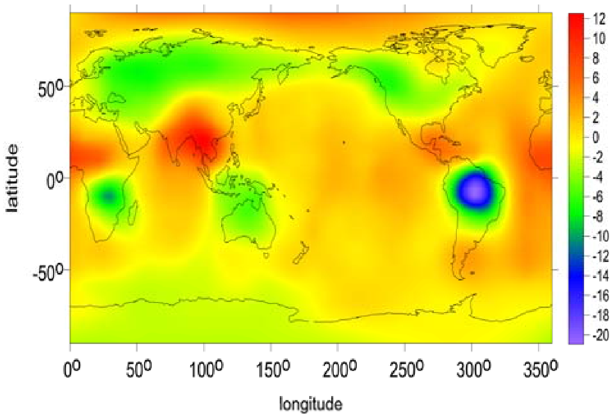

Fig. 2 Change in the geoid height [mm] between April 2002 and October 2002, based on the monthly models of CSR Texas GRACE solution.

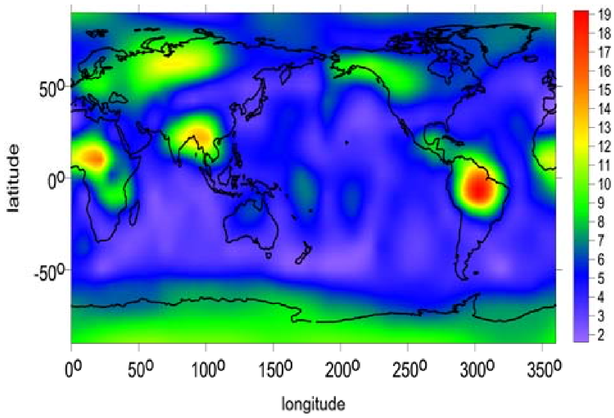

Fig. 3 Maximal change in the geoid height [mm] between May 2002 and December 2003, based on the monthly models of CSR Texas GRACE solution.

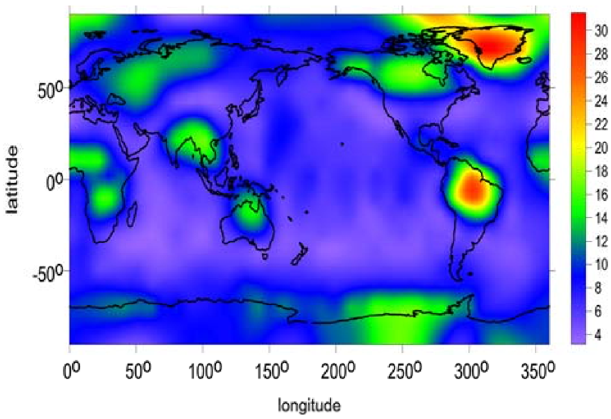

Fig. 4 Maximal seasonal changes in the geoid [mm] between 2004 and 2012 based on the monthly models of CSR Texas GRACE solution.

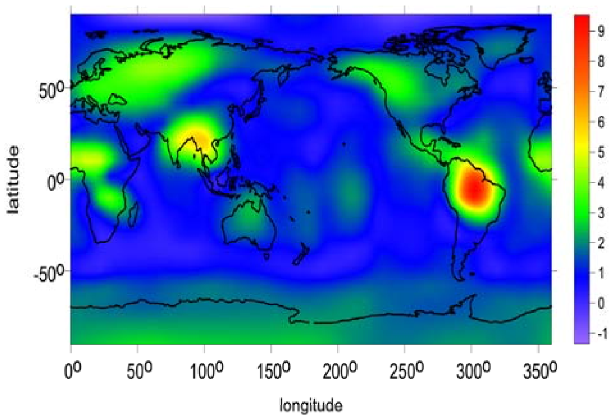

Fig. 5 Amplitudes of the seasonal change in the geoid [mm] based on the monthly models of CSR Texas GRACE solution.

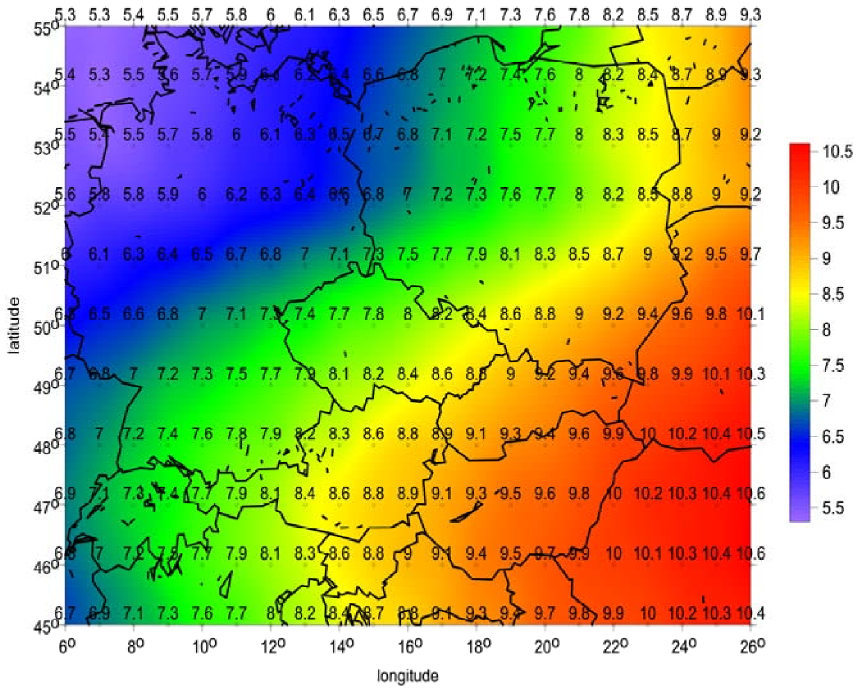

Fig. 7 Maximal change in the geoid height [mm] between 2004 and 2012, for the region of the Central Europe, based on the monthly models of CSR Texas GRACE solution.